

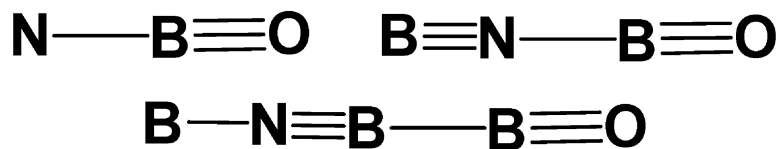
Article

Reactions of B Atoms and Clusters with NO: Experimental and Theoretical Characterization of Novel Molecules Containing B, N, and O

Mingfei Zhou, Nobuko Tsumori, Qiang Xu, Gary P. Kushto, and Lester Andrews

J. Am. Chem. Soc., **2003**, 125 (37), 11371-11378 • DOI: 10.1021/ja0367187 • Publication Date (Web): 23 August 2003

Downloaded from <http://pubs.acs.org> on March 29, 2009



More About This Article

Additional resources and features associated with this article are available within the HTML version:

- Supporting Information
- Links to the 9 articles that cite this article, as of the time of this article download
- Access to high resolution figures
- Links to articles and content related to this article
- Copyright permission to reproduce figures and/or text from this article

[View the Full Text HTML](#)



ACS Publications
High quality. High impact.

Reactions of B Atoms and Clusters with NO: Experimental and Theoretical Characterization of Novel Molecules Containing B, N, and O

Mingfei Zhou,^{*,†} Nobuko Tsumori,[‡] Qiang Xu,^{*,‡} Gary P. Kushto,[§] and Lester Andrews^{*,§}

Contribution from the Shanghai Key Laboratory of Molecular Catalysts and Innovative Materials, Department of Chemistry & Laser Chemistry Institute, Fudan University, Shanghai 200433, P. R. China, National Institute of Advanced Industrial Science and Technology (AIST), Ikeda, Osaka 563-8577, Japan, and Department of Chemistry, University of Virginia, Charlottesville, Virginia 22904

Received June 17, 2003; E-mail: mzhou@fudan.edu.cn (Zhou); q.xu@aist.go.jp (Xu); lsa@virginia.edu (Andrews)

Abstract: Reactions of boron atoms and clusters with NO molecules in solid argon have been studied using matrix isolation infrared absorption spectroscopy. The reaction products were identified by isotopic substitution (¹⁰B, ¹¹B, ¹⁵N¹⁶O, ¹⁴N¹⁸O, and mixtures) and comparison with density functional calculations of isotopic frequencies. In solid argon, boron atoms spontaneously reacted with NO to form the insertion molecule NBO. The BNBO and OBNNNO molecules were formed by the B and NO addition reactions to NBO. The linear BBNO and BBBNO nitrosyls also were formed spontaneously on annealing. These molecules photochemically rearranged to the more stable BNBO and BNBBO isomers, which have linear polyyne-like structures. The photosensitive OBNNNO molecule decomposed to form the NNBO₂ van der Waals complex. In addition, the novel OBON diradical was also formed on photolysis in high-concentration NO experiments.

Introduction

The reactions of boron atoms with small molecules such as CH₄, NH₃, C₂H₂, N₂, CO, and H₂ have led to a remarkable number of fundamental small molecules that provide new insight into the structure and bonding of boron-containing compounds.^{1–7} We have recently prepared several new boron carbonyls, BBCO, OCBBCO, and B₄(CO)₂ by the reactions of boron atoms or dimers with CO in a solid-argon matrix.^{8–10} These boron carbonyls exhibit intriguing structural and bonding properties.

Combined matrix isolation infrared absorption spectroscopy and quantum chemical computations established OCBBCO to be a linear molecule with some boron–boron triple-bond character.⁸ The B₄(CO)₂ molecule is a new aromatic σ – π diradical which favors an open-shell singlet over a triplet state.⁹ In contrast, compounds containing boron and NO are less known. However, the boron nitrosyl BNO and its isomers NBO and BON have been the subject of a number of previous theoretical investigations.^{11–14} In contrast to the nitrosyls of the heavier group 13 elements,^{15,16} BNO is a high-energy isomer. It has been shown that the BNO molecule forms in an initial step on the B + NO reaction pathway. Subsequent isomerization yields the NBO insertion molecule, which is ca. 70–80 kcal/mol lower in energy than BNO. The boron isonitrosyl, BON, was predicted to lie about 90 kcal/mol above NBO.¹⁴ No experimental results have been published on the boron nitrosyl and its isomers.

Here we report a detailed study of the reactions of boron atoms and clusters with NO in solid argon. We will show that

[†] Fudan University.

[‡] National Institute of Advanced Industrial Science and Technology (AIST).

[§] University of Virginia.

- (1) (a) Jeong, G. H.; Boucher, R.; Klabunde, K. J. *J. Am. Chem. Soc.* **1990**, *112*, 3332. (b) Hassandadeh, P.; Andrews, L. *J. Am. Chem. Soc.* **1992**, *114*, 9239. (c) Hannachi, Y.; Hassandadeh, P.; Andrews, L. *J. Phys. Chem.* **1994**, *98*, 6950. (d) Wang, Z. X.; Huang, M. B. *J. Am. Chem. Soc.* **1998**, *120*, 6758.
- (2) (a) Knight, L. B., Jr.; Herlong, J. O.; Kirk, T. J.; Arrington, C. A. *J. Chem. Phys.* **1992**, *96*, 5604. (b) Thompson, C. A.; Andrews, L. *J. Am. Chem. Soc.* **1995**, *117*, 10125. (c) Thompson, C. A.; Andrews, L.; Martin, J. M. L.; El-Yazal, J. *J. Phys. Chem.* **1995**, *99*, 13839. (d) Wang, Z. X.; Huang, M. B.; Schleyer, P. v. R. *J. Phys. Chem. A* **1999**, *103*, 6475.
- (3) (a) Martin, J. M. L.; Taylor, P. R.; Hassanzadeh, P.; Andrews, L. *J. Am. Chem. Soc.* **1993**, *115*, 2510. (b) Andrews, L.; Hassanzadeh, P.; Martin, J. M. L.; Taylor, P. R. *J. Phys. Chem.* **1993**, *97*, 5839. (c) Flores, J. R.; Largo, A. *J. Phys. Chem.* **1992**, *96*, 3015. (d) Sakai, S.; Morokuma, K. *J. Phys. Chem.* **1987**, *91*, 3661.
- (4) (a) Knight, L. B., Jr.; Hill, D. W.; Kirk, T. J.; Arrington, C. A. *J. Phys. Chem.* **1992**, *96*, 555. (b) Andrews, L.; Hassanzadeh, P.; Burkholder, T. R.; Martin, J. M. L. *J. Chem. Phys.* **1993**, *98*, 922.
- (5) Hamrick, Y. M.; Van Zee, R. J.; Godbout, J. T.; Weltner, W.; Lauerdale, W. J.; Stanton, J. F.; Bartlett, R. J. *J. Phys. Chem.* **1991**, *95*, 2840.
- (6) Burkholder, T. R.; Andrews, L. *J. Phys. Chem.* **1992**, *96*, 10195.
- (7) (a) Tague, T. J., Jr.; Andrews, L. *J. Am. Chem. Soc.* **1994**, *116*, 4970. (b) Andrews, L.; Wang, X. F. *J. Am. Chem. Soc.* **2002**, *124*, 7280.

- (8) (a) Zhou, M. F.; Tsumori, N.; Li, Z. H.; Fan, K. N.; Andrews, L.; Xu, Q. *J. Am. Chem. Soc.* **2002**, *124*, 12936. (b) Zhou, M. F.; Tsumori, N.; Andrews, L.; Xu, Q. *J. Phys. Chem. A*, **2003**, *107*, 2458.
- (9) Zhou, M. F.; Xu, Q.; Wang, Z. X.; Schleyer, P. v. R. *J. Am. Chem. Soc.* **2002**, *124*, 14854.
- (10) Zhou, M. F.; Wang, Z. X.; Schleyer, P. v. R.; Xu, Q. *ChemPhysChem* **2003**, *4*, 763.
- (11) Harrison, J. A.; Maclagan, R. G. A. R. *Chem. Phys. Lett.* **1989**, *155*, 419.
- (12) Su, S. *THEOCHEM* **1998**, *430*, 137.
- (13) Tian, W. Q.; Orlova, G.; Goddard, J. D. *Chem. Phys. Lett.* **2002**, *356*, 7.
- (14) Zhang, L. N.; Zhou, M. F. *Chem. Phys.* **2000**, *256*, 185.
- (15) (a) Andrews, L.; Zhou, M. F.; Bare, W. D. *J. Phys. Chem. A* **1998**, *102*, 5019. (b) Andrews, L.; Zhou, M. F.; Wang, X. F. *J. Phys. Chem. A* **2000**, *104*, 8475.
- (16) Orlova, G.; Goddard, J. D. *Mol. Phys.* **2002**, *100*, 483.

the NO insertion product NBO, in addition to boron nitrosyls, BBNO and BBBNO, and OBNNO and BNBO, is formed on deposition and on annealing. Photoinduced rearrangement of BBNO to BNBO and BBBNO to BNBBO and photoinduced dissociation of OBNNO to the NNBO₂ van der Waals complex are also observed. Density functional calculations are used to corroborate the experimental findings and spectral assignments and to predict the structure and bonding of the product molecules.

Experimental and Computational Methods

The apparatus and experimental methods for matrix infrared investigation of laser-ablated atom reaction products have been described in detail previously.^{17,18} Briefly, the 1064 nm fundamental of a Nd:YAG laser was focused on a rotating boron target, and the laser-ablated boron atoms and clusters were codeposited with NO in excess argon onto a CsI window cooled normally to 8 K by means of a closed-cycle helium refrigerator. The matrix gas deposition rate was typically of 3–5 mmol per hour. Natural abundance boron (¹⁰B: 19.8%, ¹¹B: 80.2%) and ¹⁰B-enriched (97%) targets were used in different experiments. Nitric oxide (Matheson), ¹⁵N¹⁶O (MSD Isotopes, 99%), and ¹⁴N¹⁸O (Isotec, 99%) were condensed, and the most volatile fraction was used to make matrix samples in argon. In general, the matrix samples were deposited for 1 h. After sample deposition, IR spectra were recorded on a BIO-RAD FTS-6000e spectrometer at 0.5 cm⁻¹ resolution using a liquid nitrogen-cooled HgCdTe (MCT) detector for the spectral range of 5000–400 cm⁻¹. Samples were subjected to broadband ($\lambda > 240$ nm) photolysis by a mercury arc (Ushio, 100 W) and annealing cycles using resistance heat.

Quantum chemical calculations were performed to predict the structures and vibrational frequencies of the observed reaction products using the Gaussian 98 program.¹⁹ The Becke three-parameter hybrid functional with the Lee–Yang–Parr correlation corrections (B3LYP) was used.^{20,21} The 6-311+G(d) basis sets were used for the B, N, and O atoms.^{22,23} Geometries were fully optimized and vibrational frequencies calculated with analytical second derivatives. Natural bonding orbital (NBO) analyses were performed to identify the bonding nature in selected product molecules.²⁴

Results

Matrix isolation studies of the boron atom–nitric oxide reaction were done over an order-of-magnitude range of NO concentrations (0.02–0.4%) with different laser powers (ranging from 5 to 15 mJ/pulse) to control the B to NO ratio in the reaction products. The infrared spectra in selected regions with ¹⁰B and 0.04% NO in argon are illustrated in Figures 1–3, and the new product absorptions are listed in Table 1. For

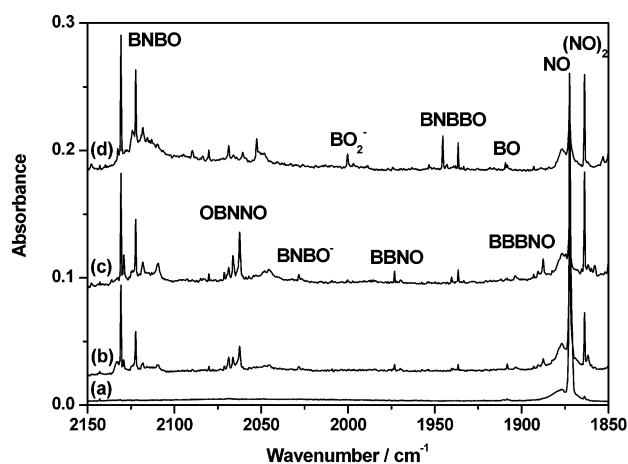


Figure 1. Infrared spectra in the 2150–1850 cm⁻¹ region from codeposition of laser-ablated boron (¹⁰B-enriched) and 0.04% NO in Ar. (a) 1 h sample deposition at 8 K, (b) after 22 K annealing, (c) after 26 K annealing, and (d) after 20 min broadband photolysis.

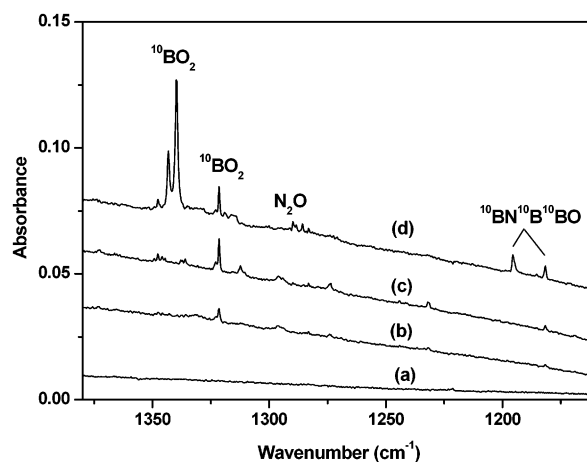


Figure 2. Infrared spectra in the 1380–1160 cm⁻¹ region from codeposition of laser-ablated boron (¹⁰B-enriched) and 0.04% NO in Ar. (a) 1 h sample deposition at 8 K, (b) after 22 K annealing, (c) after 26 K annealing, and (d) after 20 min broadband photolysis.

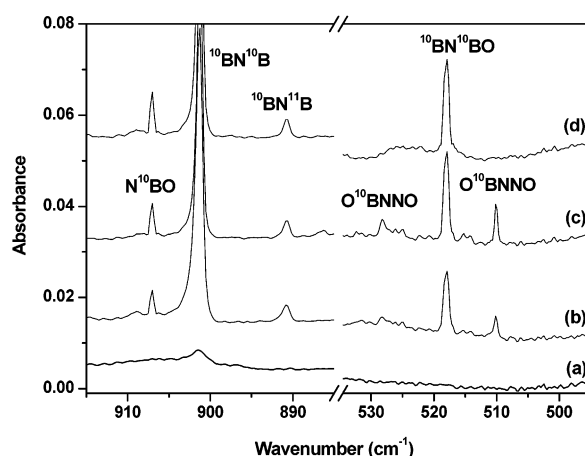


Figure 3. Infrared spectra in the 915–885 and 535–495 cm⁻¹ regions from codeposition of laser-ablated boron (¹⁰B-enriched) and 0.04% NO in Ar. (a) 1 h sample deposition at 8 K, (b) after 22 K annealing, (c) after 26 K annealing, and (d) after 20 min broadband photolysis.

comparison, the spectra in the 2150–1550 cm⁻¹ region with ¹⁰B and 0.4% NO in argon are shown in Figure 4. The stepwise annealing and photolysis behavior of the product absorptions

- (17) Burkholder, T. R.; Andrews, L. *J. Chem. Phys.* **1991**, *95*, 8697.
 (18) (a) Zhou, M. F.; Zhang, L. N.; Qin, Q. Z. *J. Am. Chem. Soc.* **2000**, *122*, 4483. (b) Chen, M. H.; Wang, X. F.; Zhang, L. N.; Yu, M.; Qin, Q. Z. *Chem. Phys.* **1999**, *242*, 81.
 (19) Frisch, M. J.; Trucks, G. W.; Schlegel, H. B.; Scuseria, G. E.; Robb, M. A.; Cheeseman, J. R.; Zakrzewski, V. G.; Montgomery, J. A., Jr.; Stratmann, R. E.; Burant, J. C.; Dapprich, S.; Millam, J. M.; Daniels, A. D.; Kudin, K. N.; Strain, M. C.; Farkas, O.; Tomasi, J.; Barone, V.; Cossi, M.; Cammi, R.; Mennucci, B.; Pomelli, C.; Adamo, C.; Clifford, S.; Ochterski, J.; Petersson, G. A.; Ayala, P. Y.; Cui, Q.; Morokuma, K.; Malick, D. K.; Rabuck, A. D.; Raghavachari, K.; Foresman, J. B.; Cioslowski, J.; Ortiz, J. V.; Stefanov, B. B.; Liu, G.; Liashenko, A.; Piskorz, P.; Komaromi, I.; Gomperts, R.; Martin, R. L.; Fox, D. J.; Keith, T.; Al-Laham, M. A.; Peng, C. Y.; Nanayakkara, A.; Gonzalez, C.; Challacombe, M.; Gill, P. M. W.; Johnson, B. G.; Chen, W.; Wong, M. W.; Andres, J. L.; Head-Gordon, M.; Replogle, E. S.; Pople, J. A. *Gaussian 98*, revision A.7; Gaussian, Inc.: Pittsburgh, PA, 1998.
 (20) Becke, A. D. *J. Chem. Phys.* **1993**, *98*, 5648.
 (21) Lee, C.; Yang, E.; Parr, R. G. *Phys. Rev. B* **1988**, *37*, 785.
 (22) (a) McLean, A. D.; Chandler, G. S. *J. Chem. Phys.* **1980**, *72*, 5639. (b) Krishnan, R.; Binkley, J. S.; Seeger, R.; Pople, J. A. *J. Chem. Phys.* **1980**, *72*, 650.
 (23) (a) Wachter, J. H. *J. Chem. Phys.* **1970**, *52*, 1033. (b) Hay, P. J.; Wadt, W. R. *J. Chem. Phys.* **1985**, *82*, 299.
 (24) Carpenter, J. E.; Weinhold, F. *THEOCHEM* **1988**, *169*, 41.

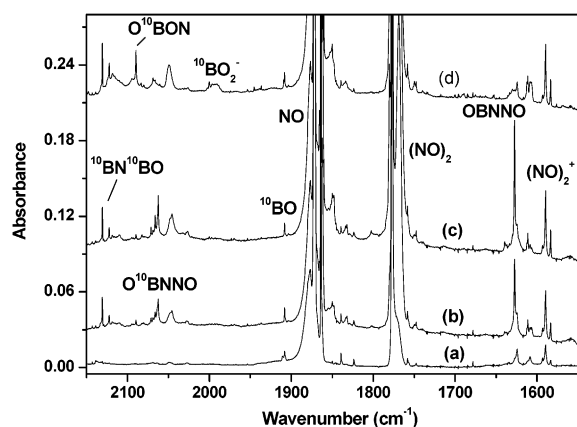


Figure 4. Infrared spectra in the 2150–1550 cm^{-1} region from codeposition of laser-ablated boron (^{10}B -enriched) and 0.4% NO in Ar. (a) 1 h sample deposition at 8 K, (b) after 22 K annealing, (c) after 26 K annealing, and (d) after 20 min broadband photolysis.

Table 1. Infrared Absorptions (cm^{-1}) from Codeposition of Laser-Ablated B with NO in Solid Argon

^{10}B			^{11}B			assignment
$^{14}\text{N}^{16}\text{O}$	$^{15}\text{N}^{16}\text{O}$	$^{14}\text{N}^{18}\text{O}$	$^{14}\text{N}^{16}\text{O}$	$^{15}\text{N}^{16}\text{O}$	$^{14}\text{N}^{18}\text{O}$	
907.0	891.7	894.0	897.4	880.9	884.3	NBO asym str
2062.3	2061.5	2033.7	1997.4	1996.1	1967.4	OBNNO B–O str
1627.4	1588.3	1605.9	1627.4	1588.3	1605.9	OBNNO N–O str
528.1	525.2	524.8	510.9	507.6	507.5	OBNNO in-plane bend
510.2	507.4	506.8	493.5	490.6	489.9	OBNNO out-of-plane bend
1339.7	1339.7	1321.6	1291.4	1291.4	1272.8	NNBO ₂ OBO asym str
2089.6	2088.4	2062.6	2029.9	2026.0	1989.6	OBON B–O str
1151.2	1139.9	1111.8	1148.6	1136.2	1108.5	OBON N–O str
2130.7	2117.4	2115.1	2068.8	2052.6	2054.1	BNBO BO str
518.0	515.3	514.8	500.7	497.9	497.3	BNBO bend
2028.2	2017.5	2013.2	1965.4	1953.5	1950.8	BNBO ⁻ BO str
1973.0	1939.1	1963.3	1943.0	1906.4	1930.9	BBNO NO str
1887.6	1854.4	1878.9	1859.5	1823.9	1848.5	BBBNO NO str
1513.3	1507.2	1496.0	1465.0	1461.1	1448.1	BBBNO BB str
1936.5	1916.3	1918.0	1889.4	1869.0	1869.1	BNBBO sym str
1181.7	1175.3	1179.8	1138.0	1131.8	1135.7	BNBBO BB str

are also shown and will be discussed below. Besides the absorptions listed in the table, absorptions are also observed for N_2O , NO_2 , $(\text{NO})_2^+$, $(\text{NO})_2^-$, BO , BO_2 , BO_2^- , BOB , and BNB .^{4,18,25} Natural abundance boron, different isotopic $^{15}\text{N}^{16}\text{O}$ and $^{14}\text{N}^{18}\text{O}$ nitric oxides, and the $^{14}\text{N}^{16}\text{O} + ^{15}\text{N}^{16}\text{O}$ and $^{14}\text{N}^{16}\text{O} + ^{14}\text{N}^{18}\text{O}$ mixtures were employed for product identification through isotopic shifts and splittings. The spectra in selected regions using these isotopic counterparts are shown in Figures

(25) Andrews, L.; Zhou, M. F.; Willson, S. P.; Kushto, G. P. *J. Chem. Phys.* **1998**, *109*, 177 and references therein.

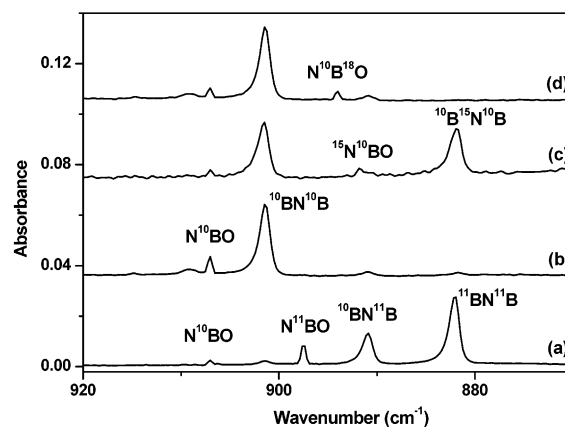


Figure 5. Infrared spectra in the 920–870 cm^{-1} region from codeposition of laser-ablated boron and NO in excess argon. (a) Natural abundance boron, 0.04% $^{14}\text{N}^{16}\text{O}$, (b) ^{10}B , 0.04% $^{14}\text{N}^{16}\text{O}$, (c) ^{10}B , 0.025% $^{14}\text{N}^{16}\text{O} + 0.025\%$ $^{15}\text{N}^{16}\text{O}$, and (d) ^{10}B , 0.025% $^{14}\text{N}^{16}\text{O} + 0.025\%$ $^{14}\text{N}^{18}\text{O}$.

5–11, respectively. The product bands reported here all show boron, nitrogen, and oxygen isotopic displacements as reported in Table 1.

Density functional calculations were performed on the potential product molecules. The optimized structures are shown in Figure 12, and the vibrational frequencies and intensities are listed in Table 2. Table 3 provides a comparison between observed and calculated isotopic frequency ratios for the observed vibrational modes.

Discussion

The new reaction product molecules will be identified from infrared spectra of isotopic mixtures and DFT calculations of isotopic frequencies.

NBO. In natural abundance boron experiments, absorptions at 907.0 and 897.4 cm^{-1} appeared together on annealing. The upper band is about 25% intensity of the lower band, which clearly indicates that only one boron atom is involved in this mode. When the ^{10}B -enriched boron target was used, only the 907.0 cm^{-1} band was observed. These two bands shifted to 891.7 and 880.9 cm^{-1} with $^{15}\text{N}^{16}\text{O}$ and to 894.0 and 884.3 cm^{-1} with $^{14}\text{N}^{18}\text{O}$. The mixed $^{14}\text{N}^{16}\text{O} + ^{15}\text{N}^{16}\text{O}$ and $^{14}\text{N}^{16}\text{O} + ^{14}\text{N}^{18}\text{O}$ spectra (Figure 5) clearly indicate that only one N and one O atom are involved in the mode. These two bands are assigned to the N^{10}BO and N^{11}BO isotopomers.

The geometry and vibrational frequencies of four different geometric BNO isomers have been recently addressed by using different DFT and MP2 methods.¹⁴ The most stable NBO isomer was predicted to have a triplet ground state with a linear structure. The B3LYP/6-311+G*-level calculations predicted the B–O and B–N stretching and the bending frequencies at 1895.7, 913.6, and 395.4 cm^{-1} for N^{11}BO . The two stretching modes are strongly coupled and, therefore, are better described as the symmetric and antisymmetric stretching vibrations. The bending frequency is out of the detection range of our IR spectrometer, while the symmetric stretching mode was predicted to have zero IR intensity. The antisymmetric stretching frequency is in good agreement with the observed value. The NBO molecule is isoelectronic with ketenylidene (CCO), which has a triplet ground state with linear geometry.²⁶ The triplet ground state NBO molecule can also be regarded as a diradical,

(26) Devilliers, C.; Ramsay, D. A. *Can. J. Phys.* **1971**, *49*, 2839.

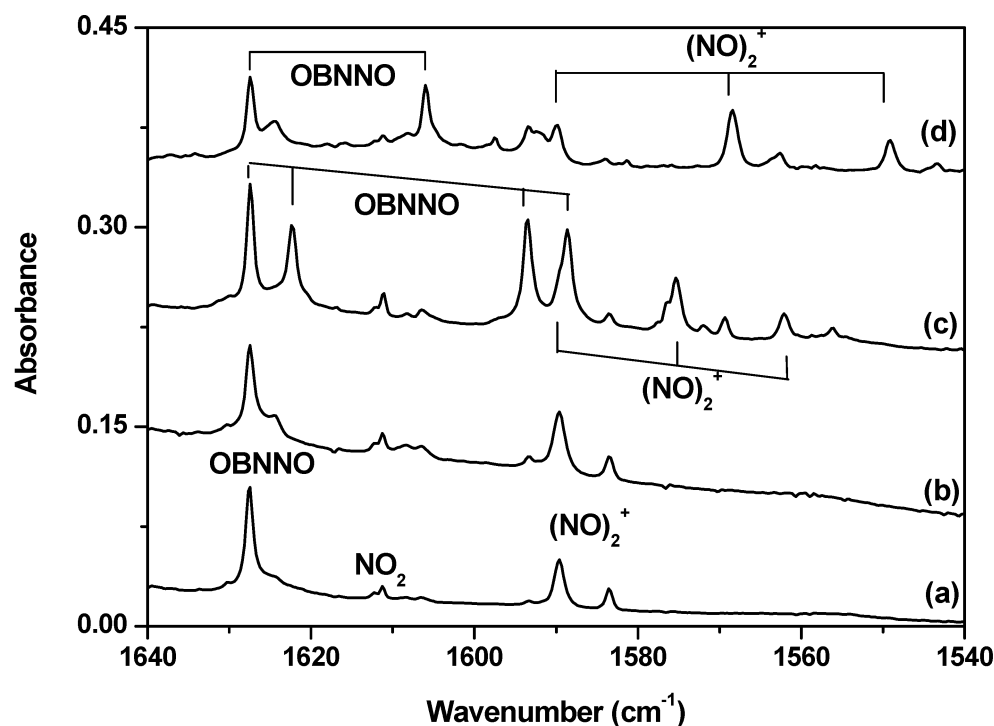


Figure 6. Infrared spectra in the 1640–1540 cm^{-1} region from codeposition of laser-ablated boron and NO in excess argon. (a) Natural abundance boron, 0.4% $^{14}\text{N}^{16}\text{O}$, (b) ^{10}B , 0.4% $^{14}\text{N}^{16}\text{O}$, (c) ^{10}B , 0.2% $^{14}\text{N}^{16}\text{O}$ + 0.2% $^{15}\text{N}^{16}\text{O}$, and (d) ^{10}B , 0.2% $^{14}\text{N}^{16}\text{O}$ + 0.2% $^{14}\text{N}^{18}\text{O}$.

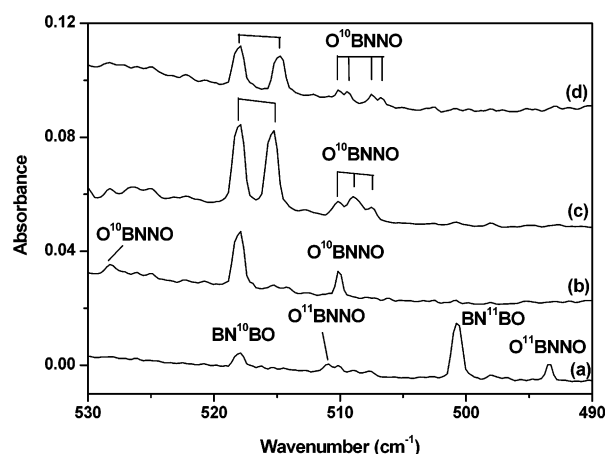


Figure 7. Infrared spectra in the 530–490 cm^{-1} region from codeposition of laser-ablated boron and NO in excess argon. (a) Natural abundance boron, 0.04% $^{14}\text{N}^{16}\text{O}$, (b) ^{10}B , 0.04% $^{14}\text{N}^{16}\text{O}$, (c) ^{10}B , 0.025% $^{14}\text{N}^{16}\text{O}$ + 0.025% $^{15}\text{N}^{16}\text{O}$, and (d) ^{10}B , 0.025% $^{14}\text{N}^{16}\text{O}$ + 0.025% $^{14}\text{N}^{18}\text{O}$.

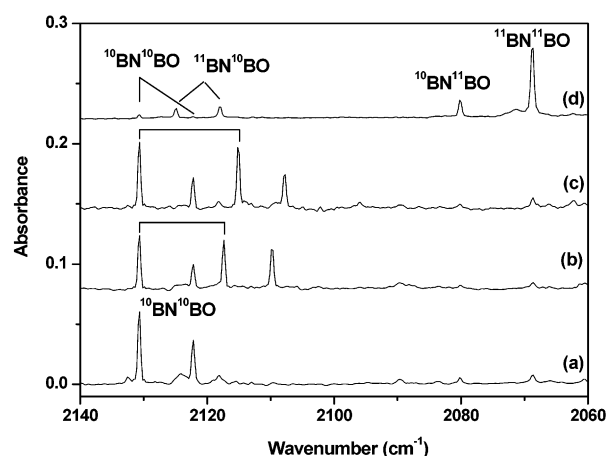


Figure 8. Infrared spectra in the 2140–2060 cm^{-1} region from codeposition of laser-ablated boron and NO in excess argon. (a) ^{10}B , 0.04% $^{14}\text{N}^{16}\text{O}$, (b) ^{10}B , 0.025% $^{14}\text{N}^{16}\text{O}$ + 0.025% $^{15}\text{N}^{16}\text{O}$, (c) ^{10}B , 0.025% $^{14}\text{N}^{16}\text{O}$ + 0.025% $^{14}\text{N}^{18}\text{O}$, and (d) natural abundance boron, 0.04% $^{14}\text{N}^{16}\text{O}$.

for which the spin density is mainly located on the N atom.¹⁴ The Lewis structure can be drawn as $\text{N}=\text{B}=\text{O}$, which satisfies the valence of B.

OBNNO. Absorptions at 2062.3, 1627.4, 528.1, and 510.2 cm^{-1} in the ^{10}B experiments increased together on annealing and were destroyed on photolysis (Figures 1 and 3). These bands are assigned to the OBNNO molecule. The 2062.3 cm^{-1} band splits into a doublet at 2062.3 and 1997.4 cm^{-1} with approximately 1:4 relative intensities in the natural abundance boron experiments, which characterizes the vibration of one boron atom. The isotopic $^{10}\text{B}/^{11}\text{B}$ ratio of 1.0325 and the $^{16}\text{O}/^{18}\text{O}$ ratio of 1.0141 (^{10}B) indicate that this mode is a B–O stretching vibration. The 1627.4 cm^{-1} band shows no boron isotopic shift. It shifted to 1588.3 cm^{-1} with $^{15}\text{N}^{16}\text{O}$ and to 1605.9 cm^{-1} with $^{14}\text{N}^{18}\text{O}$. These values give the isotopic $^{14}\text{N}/$

^{15}N ratio of 1.0246 and $^{16}\text{O}/^{18}\text{O}$ ratio of 1.0134, significantly larger and smaller than the ratios of diatomic NO, suggesting a N–O stretching vibration with strong coupling with another N atom. The mixed $^{14}\text{N}^{16}\text{O}$ + $^{15}\text{N}^{16}\text{O}$ isotopic spectrum (Figure 6) reveals a quartet at 1627.4, 1622.4, 1593.4, and 1588.3 cm^{-1} , which shows that this vibration involves two inequivalent N atoms. The mixed $^{14}\text{N}^{16}\text{O}$ + $^{14}\text{N}^{18}\text{O}$ isotopic spectrum reveals only two isotopic bands and indicates the involvement of one O atom. These data point to the involvement of a B–O subunit and a NNO subunit in the molecule. The 528.1 and 510.2 cm^{-1} bands are assigned to the in-plane and out-of-plane bending vibrations of the OBNNO molecule based on their isotopic frequency shifts (Table 1).

The assignment is strongly supported by the density functional calculations. As shown in Figure 12, the molecule was predicted

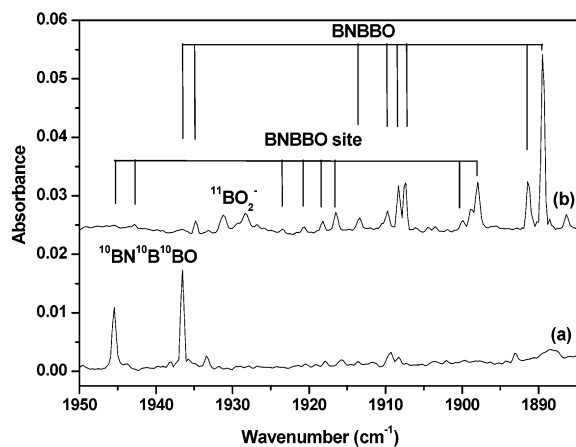


Figure 9. Infrared spectra in the 1950–1885 cm^{-1} region from codeposition of laser-ablated boron and NO in argon (after 20 min photolysis). (a) ^{10}B and (b) natural abundance boron.

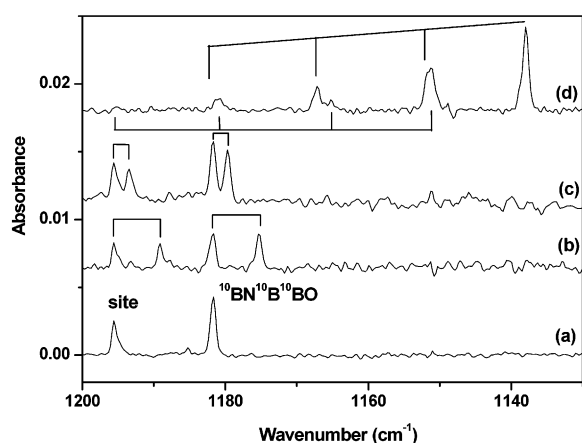


Figure 10. Infrared spectra in the 1200–1130 cm^{-1} region from codeposition of laser-ablated boron and NO in excess argon (after 20 min photolysis). (a) ^{10}B , 0.04% $^{14}\text{N}^{16}\text{O}$, (b) ^{10}B , 0.025% $^{14}\text{N}^{16}\text{O}$ + 0.025% $^{15}\text{N}^{16}\text{O}$, (c) ^{10}B , 0.025% $^{14}\text{N}^{16}\text{O}$ + 0.025% $^{14}\text{N}^{18}\text{O}$, and (d) natural abundance boron, 0.04% $^{14}\text{N}^{16}\text{O}$.

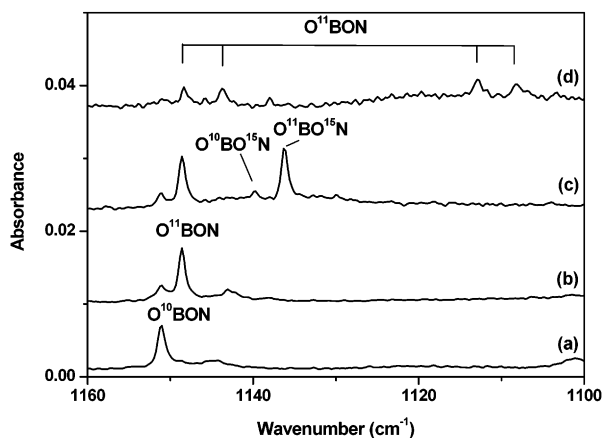


Figure 11. Infrared spectra in the 1160–1100 cm^{-1} region from codeposition of laser-ablated boron and NO in excess argon (after 20 min photolysis). (a) ^{10}B , 0.4% $^{14}\text{N}^{16}\text{O}$, (b) natural abundance boron, 0.4% NO, (c) natural abundance boron, 0.2% $^{14}\text{N}^{16}\text{O}$ + 0.2% $^{15}\text{N}^{16}\text{O}$, and (d) natural abundance boron, 0.2% $^{14}\text{N}^{16}\text{O}$ + 0.2% $^{14}\text{N}^{18}\text{O}$.

to have a $^2\text{A}'$ ground state with a bent structure. The B–O and N–O stretching and the bending vibrational frequencies for O^{11}BNNO were predicted at 2050.1, 1718.7, 524.8, and 508.6 cm^{-1} , respectively. These modes were calculated to be intense (Table

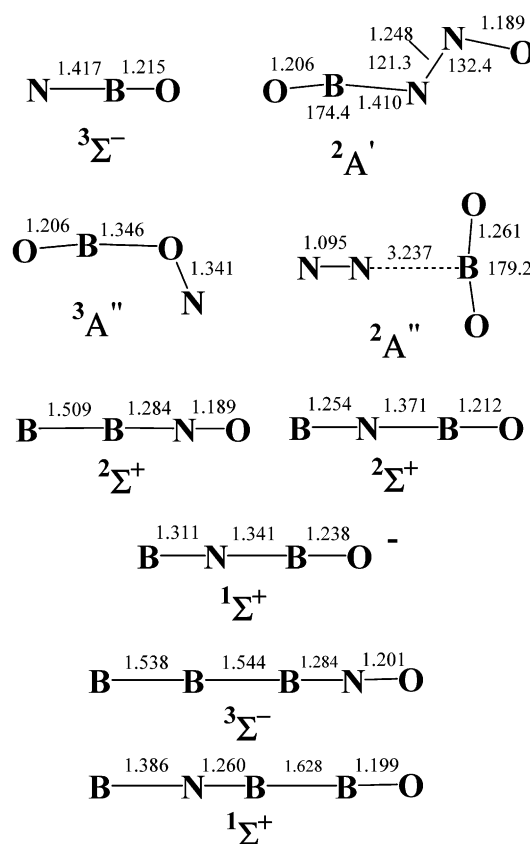


Figure 12. Optimized structures of the product molecules (bond length in Å, bond angle in degree).

Table 2. Calculated Total Energies (After Zero-Point Energy Corrections, in Hartree), Vibrational Frequencies (cm^{-1}), and Intensities (km/mol) for the Product Molecules (^{11}B)

molecule	total energy	frequency (intensity, mode)
NBO	−154.80395	1895.7 (0, σ), 913.6 (22, σ), 395.4 (140, π)
OBNNO	−284.82401	2050.1 (431, a'), 1718.7 (682, a'), 1403.4 (10, a'), 949.2 (8, a'), 602.5 (8, a'), 524.8 (39, a'), 508.6 (44, a''), 209.2 (17, a''), 161.0 (9, a')
NNBO ₂	−284.90747	2446.3 (0, a'), 1470.8 (458, a''), 1088.6 (0.1, a'), 505.2 (77, a'), 422.2 (89, a'), 67.9 (0.2, a''), 56.5 (0.2, a'), 27.3 (0.1, a''), 13.8 (0, a')
OBON	−230.04541	2073.2 (493, a'), 1191.8 (231, a'), 877.1 (14, a'), 544.8 (37, a'), 478.5 (63, a''), 193.8 (12, a')
BBNO	−179.50497	2020.3 (1103, σ), 1529.6 (6, σ), 801.0 (27, σ), 477.7 (2, π), 165.1 (1, π)
BNBO	−179.72395	2119.5 (886, σ), 1893.4 (2, σ), 861.7 (1, σ), 514.4 (124, π), 168.6 (2, π)
BNBO [−]	−179.84034	2014.3 (1587, σ), 1661.2 (72, σ), 860.7 (2, σ), 543.6 (102, π), 123.0 (51, π)
BBBNO	−204.30797	1911.0 (473, σ), 1490.7 (342, σ), 1193.5 (2, σ), 570.0 (10, σ), 444.7 (1, π), 317.2 (1, π), 114.8 (1, π)
BNBBO	−204.56651	2115.1 (91, σ), 1948.2 (888, σ), 1163.5 (243, σ), 547.0 (3, σ), 495.6 (1, π), 225.0 (46, π), 88.0 (52, π)

2). As listed in Table 3, the boron, nitrogen, and oxygen isotopic shifts also were predicted correctly.

BBNO. The 1973.0 cm^{-1} absorption appeared on annealing and decreased on photolysis (Figure 1). This band is favored in low NO concentration and high laser power experiments and is assigned to the BBNO molecule on the basis of isotopic

Table 3. Comparison between the Observed and Calculated Isotopic Frequency Ratios for the Product Molecules

molecule	mode	$^{10}\text{B}/^{11}\text{B}$		$^{14}\text{N}/^{15}\text{N}$		$^{16}\text{O}/^{18}\text{O}$	
		calcd	obsd	calcd	obsd	calcd	obsd
NBO	asym str	1.0028	1.0107	1.0220	1.0187	1.0177	1.0148
	BO str	1.0337	1.0325	1.0010	1.0007	1.0159	1.0152
OBNNO	NO str	1.0000	1.0000	1.0255	1.0246	1.0136	1.0134
	bending ^a	1.0337	1.0337	1.0061	1.0065	1.0071	1.0067
	bending ^b	1.0344	1.0338	1.0057	1.0059	1.0073	1.0073
OBON	BO str	1.0345	1.0294	1.0000	1.0019	1.0168	1.0203
	NO str	1.0001	1.0023	1.0115	1.0109	1.0375	1.0362
BBNO	NO str	1.0155	1.0154	1.0197	1.0192	1.0068	1.0063
	BO str	1.0298	1.0299	1.0082	1.0079	1.0071	1.0072
BNBO	bending	1.0342	1.0346	1.0061	1.0056	1.0067	1.0068
	BO str	1.0322	1.0320	1.0067	1.0061	1.0073	1.0075
BBBNO	NO str	1.0154	1.0151	1.0204	1.0195	1.0058	1.0060
	BB str	1.0340	1.0330	1.0026	1.0027	1.0118	1.0117
BNBBO	sym str	1.0250	1.0249	1.0116	1.0109	1.0106	1.0109
	BB str	1.0401	1.0384	1.0050	1.0055	1.0016	1.0020

^a In-plane bending. ^b Out-of-plane bending.

substitutions. In natural abundance boron experiments, a quartet at 1973.0, 1972.0, 1944.0, and 1943.0 cm^{-1} with approximately 1:4:4:16 relative intensities was observed, while in the mixed $^{14}\text{N}^{16}\text{O} + ^{15}\text{N}^{16}\text{O}$ and $^{14}\text{N}^{16}\text{O} + ^{14}\text{N}^{18}\text{O}$ experiments, only pure isotopic counterparts were presented. These data indicate that the molecule involves two inequivalent B atoms and one N atom and one O atom. The band position and isotopic frequency ratios (Table 3) are indicative of a terminal BN–O stretching vibration.

The BBNO molecule was predicted to have a doublet ground state with a linear structure (Figure 12). The B3LYP/6-311+G* harmonic frequency analysis indicates that the NO stretching mode has the largest IR intensity (1103 km/mol , versus less than 27 km/mol for the other vibrational modes). The frequency of the NO stretching mode in $^{11}\text{B}^{11}\text{B}^{14}\text{N}^{16}\text{O}$, 2020.3 cm^{-1} , is in good agreement with the experimental value. The boron, nitrogen, and oxygen isotopic frequency ratios also were predicted correctly (Table 3). In $2\Sigma^+$ BBNO, the computed B–B bond length, 1.509 Å, is about the same as the formal BB double bond of HBBH²⁷ and is slightly longer than the BB length of 1.499 Å in BBCO.¹⁰ The NO bond length is elongated from 1.148 Å in free NO to 1.189 Å in BBNO. The binding energy of BBNO with respect to ground-state B_2 ($^3\Sigma_g^-$)²⁸ and NO ($^2\Pi$) was predicted to be 96.0 kcal/mol , significantly higher than that of BBCO (66.9 kcal/mol).¹⁰

BNBO. The present experiments provide evidence for other products of the B_2NO stoichiometry. The strong bands at 2130.7 and 518.0 cm^{-1} increased markedly on annealing and slightly increased on photolysis (Figures 1 and 3) and are assigned to the B–O stretching and bending vibrations of BNBO. The natural abundance boron experiments and the mixed $^{14}\text{N}^{16}\text{O} + ^{15}\text{N}^{16}\text{O}$ and $^{14}\text{N}^{16}\text{O} + ^{14}\text{N}^{18}\text{O}$ experiments (Figures 7 and 8) clearly indicate that two inequivalent B atoms, one N atom, and one O atom are involved in the molecule. For the upper mode, two bands were observed for the $^{10}\text{B}^{10}\text{B}^{10}\text{O}$ and $^{11}\text{B}^{10}\text{B}^{10}\text{O}$ isotopomers, whereas only one band was observed for the $^{10}\text{B}^{11}\text{B}^{10}\text{O}$ and $^{11}\text{B}^{11}\text{B}^{10}\text{O}$ isotopomers. This suggests that the B–O stretching mode of the $^{10}\text{B}^{10}\text{B}^{10}\text{O}$ and $^{11}\text{B}^{10}\text{B}^{10}\text{O}$ isotopomers is in an anharmonic resonance with a combination of lower-lying levels.

- (27) (a) Breboux, G.; Barthelat, J. C. *J. Am. Chem. Soc.* **1993**, *115*, 4870. (b) Knight, L. B., Jr.; Kerr, K.; Miller, P. K.; Arrington, C. A. *J. Phys. Chem.* **1995**, *99*, 16842.
 (28) (a) Langhoff, S. R.; Bauschlicher, C. W. *J. Chem. Phys.* **1991**, *95*, 5882. (b) Bruna, P. J.; Wright, J. S. *J. Phys. Chem.* **1990**, *94*, 1774.

The calculated frequencies at the optimized geometry of BNBO provide excellent support for the assignment. The two experimentally observed modes were calculated at 2119.5 and 514.4 cm^{-1} in $^{11}\text{B}^{14}\text{N}^{11}\text{B}^{16}\text{O}$, just 50.7 and 13.7 cm^{-1} from the observed values (2068.8 and 500.7 cm^{-1} , respectively). Both of these modes were predicted to be intense (886 and 124 km/mol ; the other modes have intensities less than 2 km/mol). The boron, nitrogen, and oxygen isotopic shifts also were predicted correctly (Table 3). The BNBO molecule has a linear doublet ground state (Figure 12), with the (core)⁸ $(5\sigma)^2(6\sigma)^2(7\sigma)^2(8\sigma)^2-(1\pi)^4(2\pi)^4(9\sigma)^1$ electronic configuration. The 5σ , 6σ , and 7σ MO's are B–O and two B–N σ -bonding orbitals, and the 8σ MO is nonbonding and is predominantly oxygen-based. The doubly degenerate 1π MO's are conjugated bonding π orbitals. The doubly degenerate 2π MO's are B–N and B–O bonding but BN–B antibonding orbitals. The singly occupied 9σ MO also is a nonbonding orbital and is mainly terminal B 2s orbital in character. The population analysis also shows that the spin is predominantly on the terminal boron atom. Therefore, doublet BNBO is a linear univalent radical. The calculated terminal B–N bond length, 1.254 Å in BNBO, is a formal B–N triple bond.²⁹ The Wiberg bond indices of terminal B–N and B–O and BN–B are 2.9, 2.9, and 1.0, respectively. The Lewis structure can be drawn as $\bullet\text{B}\equiv\text{N}-\text{B}\equiv\text{O}$.

BNBO⁻. A weak band at 2028.2 cm^{-1} increased on sample deposition and disappeared on broadband photolysis. This band also splits into a 1:4:4:16 quartet at 2028.2, 2026.0, 1968.8, and 1965.4 cm^{-1} with the natural abundance boron target, indicating that two inequivalent boron atoms are involved in this mode. The mixed $^{14}\text{N}^{16}\text{O} + ^{15}\text{N}^{16}\text{O}$ and $^{14}\text{N}^{16}\text{O} + ^{14}\text{N}^{18}\text{O}$ experiments each reveal only two isotopic bands and clearly indicate that only one N atom and one O atom are involved. The boron, nitrogen, and oxygen isotopic ratios (Table 3) are very similar to those for the B–O stretching mode of BNBO, which is 102.5 cm^{-1} higher. The photosensitive behavior and frequency reduction relative to BNBO strongly suggest assignment to the BNBO⁻ anion.³⁰ As has been discussed, the BNBO neutral is a univalent radical and can be regarded as a pseudohalogen, which is expected to be able to form stable anions.³¹ The BNBO⁻ anion was predicted to have a closed-shell singlet ground state with a linear structure (Figure 12) and has slightly longer B–N and B–O bond lengths than BNBO. As the extra electron is added in the nonbonding 9σ orbital of BNBO, the Lewis structure of the BNBO⁻ anion can be drawn as $\text{B}\equiv\text{N}-\text{B}\equiv\text{O}^-$, which satisfies the octet rule. The electron affinity of BNBO was estimated to be 73.0 kcal/mol (3.2 eV).

BBBNO. Two weak bands at 1887.6 and 1513.3 cm^{-1} increased together on annealing and greatly decreased on broadband photolysis. These two bands are favored in low NO concentration and high laser power experiments. The 1887.6 cm^{-1} band exhibits very similar isotopic shifts to the N–O stretching mode of BBNO observed at 1973.0 cm^{-1} , implying that the 1887.6 cm^{-1} band is also due to a N–O stretching vibration. The mixed $^{14}\text{N}^{16}\text{O} + ^{15}\text{N}^{16}\text{O}$ and $^{14}\text{N}^{16}\text{O} + ^{14}\text{N}^{18}\text{O}$

- (29) (a) Paetzold, P. *Pure Appl. Chem.* **1991**, *63*, 345. (b) Leroy, G.; Sana, M.; Wilante, C. *Theor. Chim. Acta* **1993**, *85*, 155. (c) Dill, J. D.; Schleyer, P. v. R.; Pople, J. A. *J. Am. Chem. Soc.* **1975**, *97*, 3402.
 (30) See for example: (a) Zhou, M. F.; Andrews, L. *J. Am. Chem. Soc.* **1998**, *120*, 11499. (b) Zhou, M. F.; Andrews, L. *J. Am. Chem. Soc.* **1999**, *121*, 9171.
 (31) (a) Birkenbach, L.; Kellermann, K. *Ber.* **1925**, *58B*, 786. (b) Crawford, M. J.; Klapotke, T. M.; Klufers, P.; Mayer, P.; White, P. S. *J. Am. Chem. Soc.* **2000**, *122*, 9052.

isotopic spectra only give the sum of pure isotopic bands and indicate single N and O atom involvement. The 1513.3 cm^{-1} band shows small nitrogen (6.1 cm^{-1}) and oxygen (17.3 cm^{-1}) isotopic shifts and a large boron isotopic shift (48.3 cm^{-1}), and it is largely a B–B stretching vibration. For both bands, the boron isotopic splittings cannot be resolved because of weakness. We assign it to the next higher boron cluster: B_3NO molecule.

DFT calculations were also performed to support the assignment. Two geometries were considered: a linear BBBNO structure and a C_{2v} structure with cyclic B_3 arrangement. Both structures were predicted to have triplet ground states. The $^3\Sigma^-$ state of linear BBBNO is 4.8 kcal/mol lower in energy than the triplet C_{2v} structure. The B3LYP/6-311+G* harmonic frequency analysis indicated that the NO and BB stretching modes have the largest IR intensities (762 and 296 km/mol , respectively, versus less than 25 km/mol for the other vibrational modes; see Table 2). The calculated boron, carbon, and oxygen isotopic shifts were in excellent agreement with the observed values (Table 3).

BNBBO. Split bands at 1936.5/1945.4 and 1181.7/1195.6 cm^{-1} in ^{10}B experiments are assigned to the BNBBO molecule at two trapping sites. These bands appeared together on photolysis and were strong in low concentration NO and high laser power experiments. As shown in Figures 9 and 10, in natural abundance boron experiments, both the site absorptions of the upper mode split into octets with approximately 1:4:4:4:16:16:16:64 relative intensities which clearly indicates that three inequivalent boron atoms are involved in this mode. The two site absorptions of the low mode split into quartets with approximately 1:4:4:16 relative intensities, indicating the involvement of two inequivalent boron atoms. The mixed $^{14}\text{NO} + ^{15}\text{NO}$ and $\text{N}^{16}\text{O} + \text{N}^{18}\text{O}$ spectra clearly demonstrate that only one N atom and one O atom are involved in both modes. The isotopic frequency shifts (Table 1) show that the upper mode is a symmetric stretching vibration with all five atoms involved and that the lower mode is a B–B stretching mode.

The BNBBO molecule was predicted to have a closed-shell singlet ground state with linear structure (Figure 12), which is 162.2 kcal/mol lower in energy than the ground-state BBBNO isomer. The computed vibrational frequencies (Table 2) and isotopic frequency ratios (Table 3) strongly support our experimental assignments. The ground state has a (core) $^{10}(6\sigma)^2(7\sigma)^2(8\sigma)^2(9\sigma)^2(10\sigma)^2(1\pi)^4(2\pi)^4(11\sigma)^2$ electronic configuration. The 6σ , 7σ , 8σ , and 9σ MO's are four σ -bonding orbitals. The 10σ MO is nonbonding and is predominantly oxygen-based. The doubly degenerate 1π MO's are conjugated bonding π orbitals. The doubly degenerate 2π MO's are B–N and B–O bonding but B–B antibonding orbitals. The 11σ HOMO is nonbonding, which is largely B 2s in character. Therefore, the BNBBO molecule exhibits a polyene-like structure, $\text{B}-\text{N}\equiv\text{B}-\text{B}\equiv\text{O}$. The observed vibrational frequencies and the predicted bond lengths are consistent with this structure. There is only about 86.7 cm^{-1} difference between the B–B stretching frequencies of $^{11}\text{BN}^{11}\text{B}^{11}\text{BO}$ (1138.0 cm^{-1}) and B_2 (1051.3 cm^{-1}).³² The B–B bond length of 1.628 Å is slightly longer than that of B_2 (1.59 Å).³² The BN–B (1.260 Å) and B–O (1.199 Å) bond lengths

are very close to that in BNBO. The Wiberg bond indices of terminal B–N, BN–B, B–B, and B–O are 1.0, 2.9, 1.0, and 3.0, respectively.

NNBO₂. Absorption at 1339.7 cm^{-1} was observed only after broadband photolysis. In natural abundance boron experiments, two bands were observed at 1339.7 and 1291.4 cm^{-1} with 1:4 relative intensities. Both bands exhibited no nitrogen isotopic shifts with $^{15}\text{N}^{16}\text{O}$ but shifted to 1321.6 and 1272.8 cm^{-1} using the $^{14}\text{N}^{18}\text{O}$ sample. When a 1:1 mixture of $^{14}\text{N}^{16}\text{O} + ^{14}\text{N}^{18}\text{O}$ was used, both bands led to triplets with intensity ratios of approximately 1:2:1, indicating that two equivalent O atoms are involved. The isotopic $^{16}\text{O}/^{18}\text{O}$ ratios 1.0137 and 1.0146 and $^{10}\text{B}/^{11}\text{B}$ ratio of 1.0374 are almost the same as that of BO_2 in solid argon, whereas the band positions are about 18.3 and 17.4 cm^{-1} blue-shifted from that of BO_2 .¹⁸ The 1339.7 and 1291.4 cm^{-1} bands appeared upon photolysis while the OBNNO absorptions greatly decreased. Therefore, we assign these two bands to the antisymmetric OBO stretching vibrations of the NNBO₂ complex.

Our DFT calculations on NNBO₂ predicted a van der Waals complex with a T-shaped C_{2v} symmetry (Figure 12). The B–N distance was predicted to be 3.237 Å; the bond lengths in both the N_2 and BO_2 units are very close to that of free N_2 and BO_2 molecules. The calculated antisymmetric OBO stretching vibrational frequency is slightly shifted from that of BO_2 . The N–N stretching mode has very low IR intensity (Table 2) and was not observed.

OBON. Sharp bands at 2089.6 and 1151.2 cm^{-1} appeared together after photolysis in relatively high NO concentration experiments. Both bands split into doublets at 2089.6/2029.9 and 1151.2/1148.6 cm^{-1} with intensity ratios of approximately 1:4 in natural abundance boron experiments (Figure 11), indicating that one boron atom is involved in this molecule. The upper mode shows very small nitrogen isotopic shifts. The isotopic $^{10}\text{B}/^{11}\text{B}$ and $^{16}\text{O}/^{18}\text{O}$ ratios (Table 3) suggest a B–O stretching vibration. The lower doublet shifted to 1139.9 and 1136.2 cm^{-1} with $^{15}\text{N}^{16}\text{O}$ and to 1111.8 and 1108.5 cm^{-1} with $^{14}\text{N}^{18}\text{O}$. These values give the isotopic $^{14}\text{N}/^{15}\text{N}$ ratios of 1.0099 and 1.0109 and $^{16}\text{O}/^{18}\text{O}$ ratios of 1.0354 and 1.0362, respectively. In the mixed $^{14}\text{N}^{16}\text{O} + ^{15}\text{N}^{16}\text{O}$ isotopic spectrum (Figure 11, trace c) only the pure isotopic counterparts were presented, while a quartet at 1148.6, 1143.7, 1112.9, and 1108.5 cm^{-1} with approximately 1:1:1:1 relative intensities was produced in the mixed $^{14}\text{N}^{16}\text{O} + ^{14}\text{N}^{18}\text{O}$ isotopic spectrum (Figure 11, trace d), indicating that this mode is mainly a N–O stretching vibration coupled with one more inequivalent O atom. The band position is too low for the terminal N–O stretching of a nitrosyl species.³³ The observed isotopic frequency ratios show less N and more O participation in this mode than the diatomic NO molecule. This suggests an isonitrosyl structural arrangement. Therefore, assignment to an OBON molecule is proposed. Further confirmation of the assignment is found in the DFT-predicted frequencies at 2073.2 and 1191.8 cm^{-1} (^{11}B) and the good agreement between the observed and calculated isotopic frequency ratios for both stretching modes of OBON (Table 3) and the lack of agreement for the OBNO isomer.

OBON is potentially a very interesting molecule. It was predicted to have a triplet ground state ($^3A''$) with a bent structure (Figure 12). The spin density is predominately located

(32) (a) Herzberg, G. *Molecular Spectra and Molecular Structure*, Vol. 1; Van Nostrand: New York, 1950. (b) Huber, K. P.; Herzberg, G. *Molecular Spectra and Molecular Structure*, Vol. 4; Van Nostrand: New York, 1979.

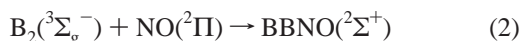
(33) Andrews, L.; Citra, A. *Chem. Rev.* **2002**, *102*, 885.

on the terminal N atom, therefore the OBON molecule is a diradical. The N–O bond length was predicted to be 1.341 Å, significantly longer than that of bent nitrosyls formally regarded as exhibiting an N–O double bond. It is a higher-energy isomer of OBNO. The ground state of OBNO was found to be a bent triplet ($^3A''$), which is 11.8 kcal/mol lower in energy than triplet OBON. No evidence was found for the OBNO molecule in the experiments.

Reaction Mechanisms The codeposition of laser-ablated boron atoms and clusters with NO in excess argon produced NBO, OBNNNO, BNBO, BBNO, and BBBNO. The NBO molecule is formally the result of the insertion of a B atom into the NO bond. There are two possible reactions to form the NBO molecule in our experiments: direct B atom insertion into the NO bond (reaction 1), which was predicted to be quite exothermic, and the reaction between BO and atomic N. The BNB, BOB, and BO absorptions were observed in the experiments, which showed that some of the NO molecules were dissociated during the ablation/condensation process. As shown in Figures 1 and 3, the NBO, BO, and BNB absorptions all increased on 22 K annealing, but the BO and BNB absorptions decreased, whereas the NBO absorption still increased on 26 K annealing. This suggests that reaction 1 does proceed in solid argon. Previous theoretical investigations showed that the BNO molecule formed in an initial step on the B + NO reaction pathway without energy barrier.¹⁴ BNO underwent molecular bending via transition state to form NBO. At the B3LYP/6-311+G* level, the transition state was predicted to be 23.7 kcal/mol higher in energy than BNO. The NO addition to form BNO is initially exothermic by 60.6 kcal/mol, which significantly surmounts the energy barrier for the isomerization reaction. The BNO molecule was not observed in the experiments, which also supports the spontaneous insertion reaction 1.



The BBNO and BBBNO nitrosyls increased on annealing in low NO concentration and high laser power experiments. These molecules were formed by addition reactions 2 and 3, which are exothermic with minimal activation energy. Both the BBCO and BBNN molecules have been observed in our previous experiments, and they both were formed from B₂ reactions in solid argon.¹⁰ The B₃ cluster also has been produced by laser evaporation and has been trapped in solid matrix.³⁴ An electron spin resonance spectroscopic study provided evidence that the ground state of B₃ is a doublet with cyclic D_{3h} symmetry, in agreement with theoretical calculations.³⁵ Binding by a NO molecule favors the linear arrangement.

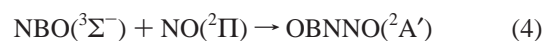


The absorptions due to the OBNNNO and BNBO molecules increased on annealing, which indicates that OBNNNO and BNBO can be formed by the simple addition reactions 4 and 5.

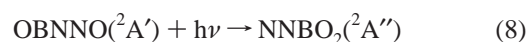
(34) (a) Hamrick, Y. M.; Van Zee, R. J.; Weltner, W., Jr. *J. Chem. Phys.* **1992**, *96*, 1767. (b) Li, S.; Van Zee, R. J.; Weltner, W., Jr. *Chem. Phys. Lett.* **1996**, *262*, 298.

(35) (a) Martin, J. M. L.; Francois, J. P.; Gijbels, R. *J. Chem. Phys.* **1989**, *90*, 6469. (b) Hanley, L.; Whitten, J. L.; Anderson, S. L. *J. Phys. Chem.* **1988**, *92*, 5803. (c) Kato, H.; Kamashita, Y.; Morokuma, K. *Chem. Phys. Lett.* **1992**, *190*, 361. (d) Boustani, I. *Phys. Rev. B* **1997**, *55*, 16426.

The observation of BBNO indicates that BNBO does not directly come from B₂ reaction. The BBNO and BBBNO absorptions decreased on photolysis, during which the BNBO and BNBBO absorptions increased. These observations suggest that BBNO and BBBNO undergo photoinduced isomerism to BNBO and BNBBO, as shown in reactions 6 and 7. Our B3LYP calculations predicted that the linear BNBO and BNBBO molecules are 137.4 and 162.2 kcal/mol more stable than the linear BBNO and BBBNO isomers. Both BNBO and BNBBO are global minima on the B₂NO and B₃NO potential energy surfaces. We also computed a number of other structural isomers with B₂NO and B₃NO formulas, such as the linear BOBN, OBNB, BNOB, and BBON, the linear BBNBO, BNBOB, BBOBN, and cyclic structural isomers of BNBBO. All of these isomers are higher in energy than BNBO and BNBBO. The linear BNBO and BNBBO arrangement is favored over the other structural isomers to maximize the B–N and B–O π bonding.



The OBNNNO molecule also is photosensitive: It decreased on broadband photolysis. In the experiments with lower NO concentrations, the dominant photolysis product is the NNBO₂ van der Waals complex. This implies photoisomerization reaction 8, which was calculated to be exothermic by 52.4 kcal/mol. In higher NO concentration experiments, the OBON diradical was formed on photolysis. It appears that this diradical was produced on photoinduced dissociation of the OBNNNO complex, reaction 9. Strong N₂O absorptions also were produced on photolysis, along with the OBON absorptions.



Conclusions

Reactions of laser-ablated boron atoms and clusters with NO molecules have been studied using matrix isolation infrared absorption spectroscopy and quantum chemical calculations. Boron atoms and clusters reacted with NO to form the NBO, OBNNNO, BBNO, BNBO, and BBBNO molecules spontaneously on annealing in solid argon. The boron nitrosyls BBNO and BBBNO are linear molecules. They underwent photochemical rearrangement to the BNBO and BNBBO molecules, which have linear polyyne-like structures. Photoinduced dissociation of OBNNNO and higher complex to the NNBO₂ van der Waals complex and the OBON diradical were also observed. Evidence is also presented for the linear BNBO⁻ anion. The aforementioned product molecules were characterized via isotopic substitution (¹⁰B, ¹¹B, ¹⁵N¹⁶O, ¹⁴N¹⁸O, and mixtures) as well as DFT isotopic frequency calculations.

Acknowledgment. This work is supported by N.S.F.C. and the N.K.B.R.S.F. of China, the N.E.D.O. of Japan, and the A.F.O.S.R. of the United States.

JA0367187